Efficient Synthesis of Fullerenol in Anion Form for the Preparation of Electrodeposited Films

Fang F. Wang, Ning Li,* Dong Tian, Guo F. Xia, and Ning Xiao

Department of Chemical Engineering and Technology, Harbin Institute of Technology, Harbin 150001, China

ARTICLE

ABSTRACT The first electrochemical characterization of the much-studied "fullerenols" has been carried out. The fullerenol was prepared by the reaction of C_{60} in deoxygenated tetrahydrofuran with an aqueous NaOH solution using sodium zincate as an electrophilic reagent. The obtained fullerenol is not simply polyhydroxylated C_{60} but is a structurally and electronically complex C_{60} anion with a molecular formula of $Na^{+}{}_2[C_{60}(OH)_{12}(O)_2]^{2-}$. This negatively charged fullerenol is in the form of a spherical cluster of 50 nm in diameter, and it can migrate in the same solution to an anode surface and be oxidized into the less soluble fullerenol $C_{60}O(OH)_{12}$, when 10 V is applied to the electroplating bath. A uniform film, with a particle of 50—250 nm in diameter and a thickness of a few 10—100s of nanometers, is obtained by drying the fullerenol covered anode. This is the first time that studies of water-soluble fullerenols acting as anions for electrodeposited film preparation have been reported. The deposition mechanism has been further demonstrated by electrochemical measurements and dissolved oxygen concentration testing to be an oxidation process consisting of two anodic oxygen evolution processes.

KEYWORDS: fullerenol · anion · film · electrodeposition · oxidation

Water-soluble fullerenols have been thought to have potential applications in a variety of areas, including optoelectronics, medical therapeutics, biochemistry, polymer materials science, and electrochemistry, owing to their unique properties.[1−4] Examples of specific applications that have incorporated fullerenol materials are polymer-based solar cells,[5,6] drug delivery agents,[7,8] antioxidants *in vivo*,[9−11] macromolecular materials,[12−14] and proton conductors.[15,16] However, information regarding the possible applications of fullerenol in electrochemistry is limited. While several methods, involving the hydrolysis of a fullerene intermediate through the use of nitronium chemistry,[17] sulfuric and nitric acid,[18,19] oleum,[20,21] nitrogen dioxide radicals,[22] hydrogen peroxide,[23,24] or polyethylene glycol (PEG400)[25,26] have been developed to synthesize water-soluble fullerenols, these methods can not be utilized in electrochemical research because of the electrical neutrality of these molecules. It is therefore of great significance to develop a novel synthetic method for production of charged water-soluble fullerene. Recently, Husebo *et al.* reported the reaction of an aqueous NaOH solution in contact with a toluene or benzene solution of C_{60} using tetrabutylammonium hydroxide (TBAH) as a phase transfer agent to prepare $Na^{+}{}_n[C_{60}O_x(OH)_y]^{n-}$. In addition, halogenated fullerenes were also used as reagents to prepare alkali metal fullerenols, which have been characterized to be stable anions in aqueous solution.[27,29−31] Such metalated fullerenols are undoubtedly the appropriate species for further study of possible electrochemical applications. However, in these attempts, fullerenes were first dissolved in a highly toxic organic solvent such as toluene or benzene or used to prepare halogenated fullerenes. Furthermore, the water-soluble fullerenols obtained in this way need to be subjected to a complicated purification process before further use. Finally, synthesis of the fullerenols has required reaction times of up to 10 h using the $C_{60(toluene)}/NaOH_{(aq)}$/TBAH method[27,28] and two weeks with the halofullerene method.[29] These have become the methods of choice for polyhydroxylation of fullerenes when only a small quantity of material is available. Therefore, a novel and efficient procedure must be developed for further electrochemical applications.

In this paper, we demonstrate the efficient synthesis and characterization of negatively charged water-soluble fullerenol prepared by the reaction of an aqueous NaOH solution mixed with the relatively nontoxic deoxygenated tetrahydrofuran (THF) solution of C_{60} with sodium zincate used as an electrophilic reagent to activate the olefinic bonds of the fullerene molecules. Furthermore, we investigate the

*Address correspondence to ffwanghit@163.com.

Received for review March 10, 2010 and accepted September 08, 2010.

Published online September 15, 2010.
10.1021/nn100485g

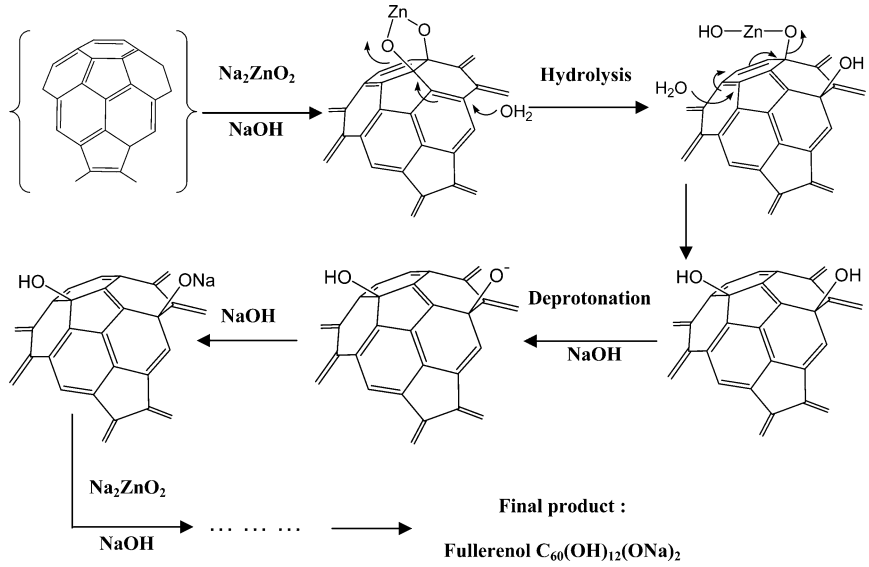

Scheme 1. Synthesis technique based upon electrophilic property of sodium zincate under strong basic conditions.

application of the fullerenol in film preparation, and the mechanism of fullerenol deposition on the anode surface.

RESULTS AND DISCUSSION

Our synthesis technique is based upon the electrophilic property of sodium zincate under strong basic conditions, as shown in Scheme 1. Freshly distilled THF was deoxygenated by purging with gaseous argon for at least 30 min. A small amount of solid C_{60} and THF were placed in a vial and sonicated under very mild conditions (90 W, 40 kHz) for 1.5−2 h at room temperature. Then, an aqueous NaOH solution, with dissolved sodium zincate, was added. Finally, this C_{60} suspension in basic solution was sonicated under the same conditions for at least 3 h. Then a standard method,[27,28,31] with slight modifications, was followed to purify the prepared fullerenol (see Experimental Section).

The FT-IR spectrum of the fullerenol sample is shown in Figure 1a. In addition to a broad O−H band centered at 3400 cm^{-1}, there are three characteristic bands at 1619, 1385, and 1051 cm^{-1}, assigned to νC═C, δ_sC−O−H, and νC−O absorption. These four broad bands are invariably reported as diagnostic absorptions from various fullerenols.[23−34] There is also a weak and unexpected band observed at 2928 cm^{-1}, indicating the possible presence of hydrogen. On prolonged standing in air (for a few months), this band disappeared, but the other bands remained effectively unaltered (Figure 1b). Such C−H stretching bands have previously been observed for fullerenols,[32−34] but more typically they are observed as the result of a tautomeric shift of hydroxyl hydrogen on the C_{60} cage. Nevertheless, the absorption bands at 527 and 775 cm^{-1} are from the C_{60} molecule cage.[35,36]

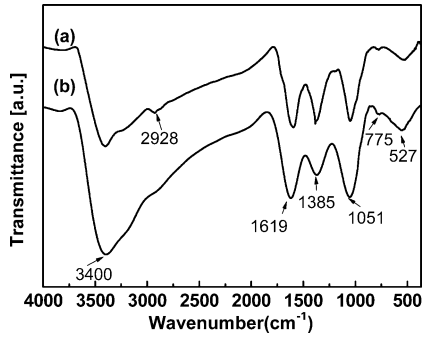

Figure 1. Infrared absorption spectrum of the fullerenol ($C_{60}(OH)_{12}(ONa)_2$) sample.

The electronic structure of fullerenol was analyzed by measuring the binding energy spectra of C_{1s}, Na_{1s}, and O_{1s} electrons. The X-ray photoelectron spectroscopy (XPS) of the C_{1s} peak is shown in Figure 2a. The fitted peak with a binding energy at 284.7 eV is assigned to nonoxidized carbon, the peak at 286.5 eV to monooxygenated carbon (C−OH) and the peak at 288.1 eV to dioxygenated carbon ($C-O^-$). In addition to the of C_{1s} peaks in the fullerenol sample (78.72 At%), Na_{1s} (2.65 At%) and O_{1s} (18.62 At%) peaks were also observed. The observation of a Na_{1s} peak at 1070.9 eV (Figure 2b) results from Na as the counterion of fullerenol. Moreover, the XPS spectrum of O_{1s} shown in Figure 2c reveals two constituents, component 1 at 531.3 eV for O−Na and component 2 at 532.5 eV for O−H. It is remarkable that the molar ratio of C, Na, and O is close to 60:2:14.

An elemental analysis of the fullerenol powder produced in this work yielded the following weight fractions: %C = 71.48, %H = 1.21%. To remove the influence of crystal water, all samples used for testing were dried at 125 °C under vacuum for 5 h. It is interesting to note that the weight fractions of C and H are close to the theoretical values (%*C* = 71.86, %*H* = 1.20%), calculated from the stoichiometry of $C_{60}(OH)_{12}(ONa)_2$. This is consistent with the conclusion obtained from the XPS analysis. Therefore, the molecular formula for the

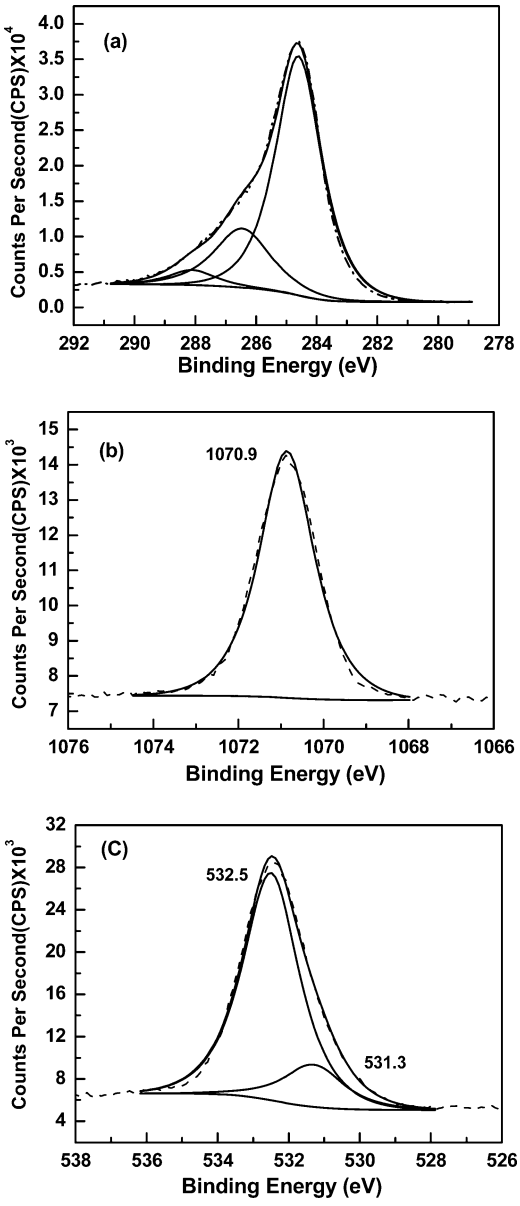

Figure 2. XPS spectrum of (a) C_{1s} binding energy of fullerenol and curve-fitting analysis showing oxidation states of carbon; (b) Na_{1s} binding energy of fullerenol; (c) O_{1s} binding energy of fullerenol.

fullerenol is confirmed to be $C_{60}(OH)_{12}(ONa)_2$ (MW = 1002 g mol^{-1}).

To further characterize the fullerenol in our present work, a time-of-flight mass spectrum measurement was performed to confirm the structure of the sample, with the result illustrated in Figure 3. The most abundant ions in this mass spectrum are centered at *m/z* 720 (relative intensity 100), corresponding to the mass of intact C_{60} ion fragments.[17,22] There are many ion clusters above *m/z* 720, clearly separated by multiples of 16 (0), 17 (OH), and 23 (Na) mass units, providing evidence of oxygen, hydroxy, and sodium entities on the fullerenol cage. This agrees well with the structure of polyhydroxylated C_{60} derivative with a molecular formula of $C_{60}(OH)_{12}(ONa)_2$.

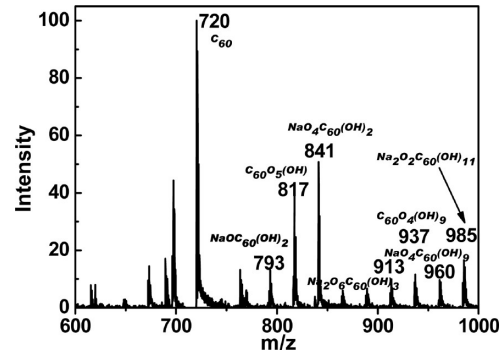

Figure 3. Time-of-flight mass spectra of direct laser-induced dissociation of the prepared fullerenol powder. All ions are negative.

The acidity of the fullerenol hydroxy groups is much higher than those of aliphatic alcohols and phenols due to the strong electron withdrawing effect of the carbon cage. Therefore, alkali metal fullerenols do not undergo hydrolysis and behave as salts and they are highly soluble in water.[29] Recently, fullerenols with similar structures have been reported to exist in anion form in aqueous solution.[27,31] In addition, the molecular formula for the fullerenol studied in this work has been confirmed to be $C_{60}(OH)_{12}(ONa)_2$ (MW = 1002 g mol^{-1}) by using XPS and elemental analysis. This indicates that Na, along with C, H, and O, is one of the four elements that made up the molecule. The fullerenol with the molecular formula $C_{60}(OH)_{12}(ONa)_2$, rather than $C_{60}(OH)_{12}(OH)_2$, has been extracted from the aqueous solution, which proved the presence of the stable RO-Na+ fullerenol structure in aqueous condition. This means that the fullerenol molecules studied in this work are negatively charged in aqueous solution with the ionic formula of $C_{60}(OH)_{12}(O^-)_2$. This property accelerates the possible application of fullerenol in the field of electrochemistry. For example, a fullerenol thin film preparation technique is developed on the basis of electrodeposition of the negatively charged fullerenol on the anode surface. The solution can be prepared by

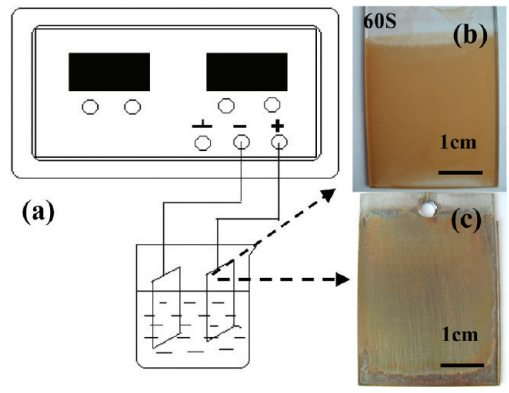

Figure 4. Preparation of C_{60} derivative films using electrodeposition technique at 10 V for 60 s (a) and their photographs: (b) film deposited on conductive glass; (c) film deposited on a thin sheet of iron. Films (b, c) were prepared from a solution of fullerenol in a complex of THF and sodium hydroxide solution with dissolved sodium zincate.

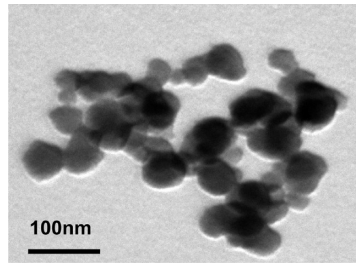

Figure 5. TEM image of the fullerenol particles in the solution at room temperature, showing the morphology of the aggregates.

the reaction of C_{60} in relatively nontoxic deoxygenated THF with an aqueous NaOH solution using sodium zincate as an electrophilic reagent, which has also been used to extract the fullerenol $C_{60}(OH)_{12}(ONa)_2$ studied in our work. As shown in Figure 4a, a FTO conductive glass and a copper sheet were immersed in the prepared solution as anode and cathode, respectively, with a voltage applied using a DC regulated power supply between the two electrodes. The deposition was performed at 10 V, and the process was usually completed within a few seconds. Subsequently, the anode was taken out from the electroplating bath and a yellow brown uniform film was found to have formed on the surface. Moreover, the films can also be deposited on other conductive substrates, such as iron, copper, graphite, and so on, by the same thin film preparation technique. Photographs of the films on a conductive glass and thin sheet of iron are shown in Figure 4b,c.

The assembly of fullerenol molecules in the solution was examined by transmission electron microscopy (TEM). The spherical assemblies, about 50 nm across, are shown in Figure 5. It is known that fullerenol molecules always aggregate into large and amorphous clusters in aqueous solution.[31,37,38] Also, the presence of short-chain groups (e.g., hydroxyl and ammonium head groups) have also been found to favor the formation of spherical clusters.[39] This aggregation phenomenon is thought to be attributed to the cohesive forces of the hydrogen-bond network. These bonds are located inside the core cluster, whereas repulsive negatively charged groups are on the outer surface of cluster. These specific features of the structure will isolate the clusters from each other in aqueous solution and make them clearly identifiable.

The films on the FTO conductive glass surface were also examined by using scanning electron microscopy (SEM). Figure 6 shows a comparison of images of the films prepared using different deposition times: (a) 20, (b) 40, and (c) 60 s. It is remarkable that not only has the surface distribution of particles changed significantly, but the diameters have decreased with increasing treatment times. As shown in Figure 6a, the deposited particles have spherical morphology and are scattered over the surface of the substrate, with diameters varying from 50 to 250 nm. A similar phenomenon is observed in Figure 6b. The appearance of the film is more uniform, and the particles are a little smaller than in Figure 6a. In addition, a well-organized film with a particle size of about 50 nm formed when the deposition time went up to 60 s (Figure 6c). Therefore, the arrangement of molecules on the film surface is highly dependent on the length of deposition time.

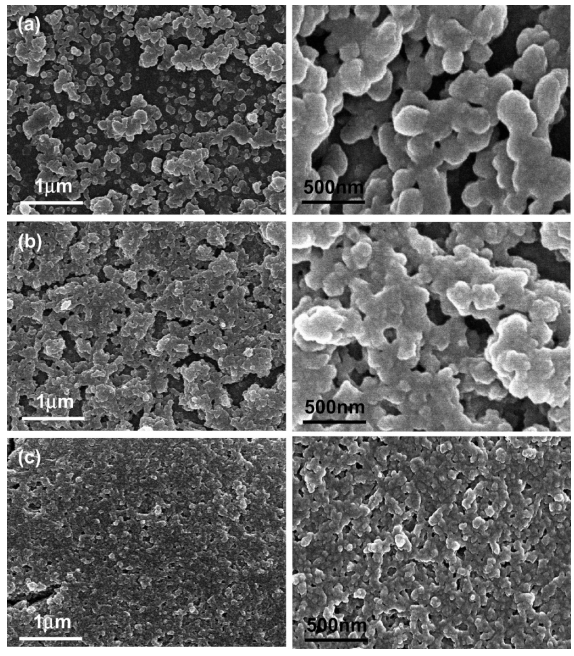

Figure 6. SEM images of the C_{60} derivative films on FTO conductive glass surface prepared using deposition time (a) 20, (b) 40, and (c) 60 s, at low and high magnification.

On both theory and empirical studies, a relatively low deposition rate can contribute to an improved surface quality of the film and a fine crystal structure. To examine the variation of current density on the anode surface, current−time measurements were performed. The current−time curve was tested with a constant 10 V between the anode and cathode in the electroplating bath. It can be seen from the curve that the oxidation current density decreases and the film resistance increases as time goes on. Therefore, this deposition time dependence of the arrangement of particles on the surface is due to increased film resistance and reduction of the deposition rate as a function of time.

The thicknesses of the films as a function of deposition time are shown in Figure 7 and confirmed by cross-sectional SEM measurements. The film thickness is highly dependent on the length of treatment time. Up to $t = 40$ s there is a clear trend of increasing film thickness as the deposition time increases, but this is reversed when the time is further prolonged ($t > 40$ s). This result shows that the film thickness is not directly proportional to the treatment time, which means that the film prepared using the electrodeposition technique can also be dissolved by the solution. Accordingly, we predict that the formation of films using electrodeposition technique is characterized by competing

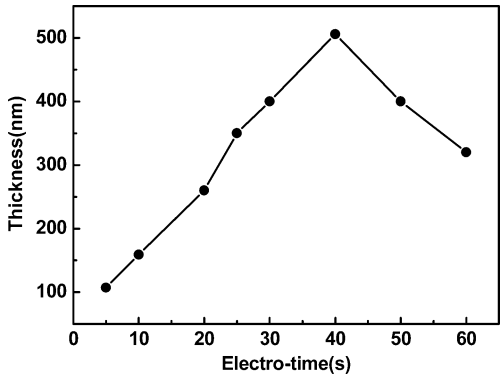

Figure 7. Thickness of film prepared using the newly developed electrodeposition technique as a function of deposition time.

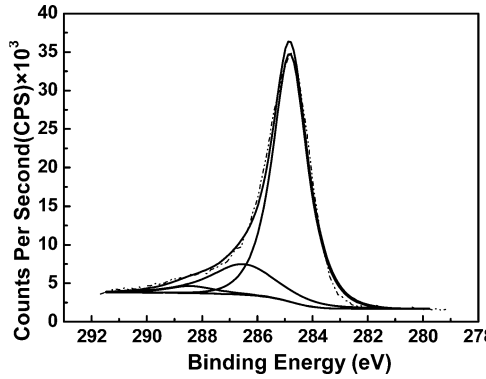

Figure 9. XPS spectrum of C_{1s} binding energy of film prepared using electrodeposition technique with oxidation states of carbon shown through curve-fitting analysis.

film deposition and dissolution processes. The film thickness increases when the deposition rate exceeds the dissolution rate of film product, otherwise the thickness decreases. It can therefore be concluded that the deposition is self-limiting and it slows down as the applied coating electrically insulates the anode, a result which is consistent with the conclusion drawn through SEM analysis.

To investigate deposition mechanisms for the fullerenol, FT-IR spectra and XPS experiments were also performed to characterize the film product. The FT-IR spectrum depicted in Figure 8 shows the characteristic features of fullerenols, namely, a broad absorption band related to the hydroxyl group and centered at 3413 cm^{-1}, a C═C band at 1618 cm^{-1}, and two C−O bands at 1386 and 1031 cm^{-1}. Two C−H stretching bands, at 2922 and 2866 cm^{-1}, can also be identified in the spectrum, just as in Figure 1a. In addition, a new band was observed at 1706 cm^{-1}, which means the presence of a hemiketal group.[18] It has been proven that this hemiketal structure of fullerenol in solution changes reversibly as a function of pH.[31]

There are changes in the position and intensity of the peaks between the two FT-IR spectra (Figure 1 and Figure 8). The hydroxyl group-related absorption band at 3400 cm^{-1} is blue-shifted to 3413 cm^{-1}, which suggests that there is a decrease in the intermolecular association originating from the hydrogen bonds of fullerenol. Another result is the presence of a down-

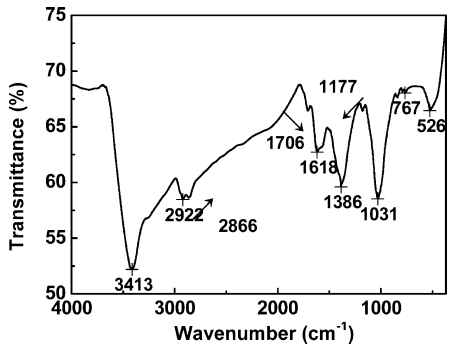

Figure 8. FT-IR absorption spectrum of the deposited film.

shift of about 20 cm^{-1} of the band associated with the C−O stretching absorption, which may originate from the reduction of the steric hindrance of hydrogen bonds. As shown in Figure 1, the C═C stretching vibration band is one of the most intense bands in the spectrum. However, in Figure 8, this band is of only moderate intensity with its frequency raised to 1618 cm^{-1}. The blue shift of the C═C stretching vibration band is ascribed to the hemiketal structure of the film product, which hinders the stretching vibration of the C═C bands. Moreover, the intensity reduction of the C═C stretching vibration band may be induced by the increasing symmetry of C═C bands and smaller dipole moment changes. These results can be explained by contributions from structural changes in the fullerenol after deposition.

The XPS of the C_{1s} peak shown in Figure 9 reveals three functional groups of the product. The fitted peak with a binding energy at 284.7 eV is assigned to nonoxidized carbon, the peak at 286.5 eV to monooxygenated carbon (C−OH), and the peak at 288.3 eV to hemiketal carbon. The XPS results are consistent with the conclusion drawn from the FT-IR analysis, which revealed characteristic features of fullerenol with hemiketal structure of the film. In addition to the C1s peaks in the fullerenol sample (82.32 At%), O1s (17.67 At%) peaks were also observed. It is significant that the molar ratio of C and O is close to the expected value of 60:13.

Furthermore, elemental analysis of the film powder yielded the following weight fractions: %C = 76.62, %H = 1.28%, %O = 22.1%. The molecular formula of the film can be calculated by using the molar ratio of C and O from the XPS measurement and the elemental analysis result. Accordingly, we deduce that the stoichiometry of the film can be written as $C_{60}O(OH)_{12}$ (MW = 940 g mol^{-1}).

The fullerenol changes its structure when it is deposited on the anode surface. To confirm if the oxidation of fullerenol takes place during deposition. The activity of fullerenol was checked using two electrochemical methods, potentiostatic and cyclic voltammetric mea-

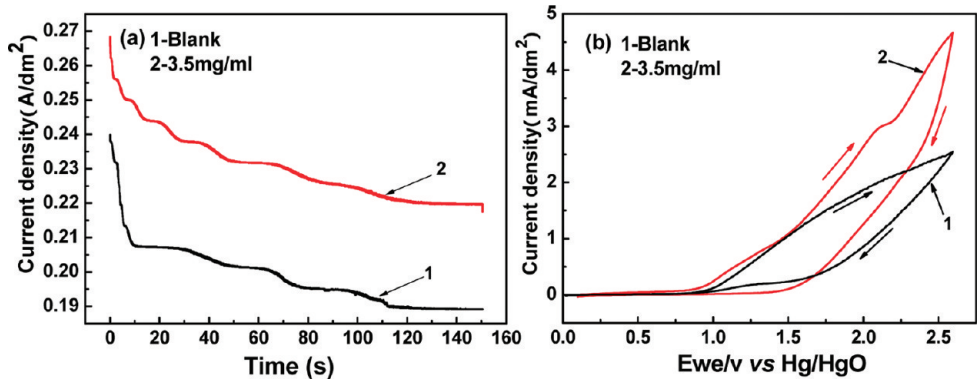

Figure 10. (a) Potentiostatic $I-t$ and (b) cyclic voltammetric curves obtained for fullerenol transferred on to FTO conductive glass anode. Current−time curves obtained with THF/aqueous NaOH solutions containing dissolved sodium zincate (5:2 by volume) at room temperature under a constant 10 V between two electrodes, with and without fullerenol $C_{60}(OH)_{12}(ONa)_2$. Cyclic voltammetric curves obtained using a 5 mV · s^{-1} scan rate for both solutions.

surements. The two methods can be applied to determine whether electrochemical reactions have occurred during the anodic deposition process. In addition, cyclic voltammetry is technique commonly used to acquire qualitative information of electrochemical reactions. It provides a rapid location of the redox potentials of electroactive species.

Potentiostatic measurements were carried out at a constant 10 V in different solutions using two electrodes, the FTO conductive glass working electrode and a platinum counter electrode. The solution was prepared by mixing THF with an aqueous NaOH solution containing dissolved sodium zincate. The mixed solution was divided into two parts. Fullerenol, synthesized through the electrophilic reaction described above, was added to the first part to achieve a concentration 3.5 mg/mL; nothing was added to the second part. The resulting curve in Figure 10a-2 reveals an obvious increase of the electric charge output ($Q = I \cdot t$) in comparison with that in Figure 10a-1, and the increase is ascribed to the discharge of fullerenol on the anode surface. So, it can be concluded that the negatively charged fullerenols lose their electrons on the anode surface during deposition.

In addition, cyclic voltammetric measurements were conducted in the same two solutions using a FTO conductive glass working electrode, a platinum counter-electrode, and an Hg/HgO reference electrode. Figure 10b shows the results obtained with and without fullerenol $C_{60}(OH)_{12}(ONa)_2$. Figure 10b-1 shows anodic evolution of oxygen from the hydroxyls. The resulting curve in Figure 10b-2 shows an additional oxidation peak at 2.15 V (vs Hg/HgO). The obvious increase of the electrical charge output shown in Figure 10a-2 and the additional oxidation peak in Figure 10b-2 confirm the oxidation of the fullerenol $C_{60}(OH)_{12}(ONa)_2$ on the anode surface during the deposition process.

To determine the mechanism of the electrodeposition process, dissolved oxygen (DO) concentration in above solutions during the deposition process was also monitored using DO tester. A FTO conductive glass and a platinum sheet were immersed in the prepared solutions as anode and cathode, respectively. The two solutions were deoxygenated by purging with gaseous argon before testing. DO concentration was measured under the protection of argon, when a voltage of 10 V was supplied. As shown in Figure 11-2, there is an obvious increase of the DO concentration in comparison with that in Figure 11-1, and the increase is attributed to the oxidation of the fullerenol $C_{60}(OH)_{12}(ONa)_2$ on the anode surface. Therefore, oxidation of the fullerenol $C_{60}(OH)_{12}(ONa)_2$ on the anode surface is an oxygen evolution process.

Based on the spectroscopic identification of the main reaction products of the film and the oxygen evolution mechanism, the following electrode reaction is proposed (eq 1). In addition, it can be seen from the curves shown in Figure 11-1 that oxidation of hydroxyls also occurs along with the deposition process and oxygen is given out. Therefore, the oxidation on the working electrode consists of two anodic oxygen evolution processes (eqs 1 and 2).

$$C_{60}(OH)_{12}(O^-)_2 - 2e^- \Rightarrow C_{60}O(OH)_{12} + \frac{1}{2}O_2\uparrow \quad (1)$$

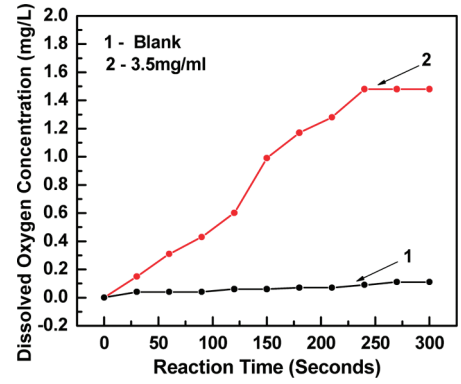

Figure 11. Dissolved oxygen concentration in the solutions during the deposition process. Curves obtained with THF/aqueous NaOH solutions containing dissolved sodium zincate (5:2 by volume) at room temperature under a constant 10 V between two electrodes, with and without fullerenol $C60(OH)_{12}(ONa)_2$.

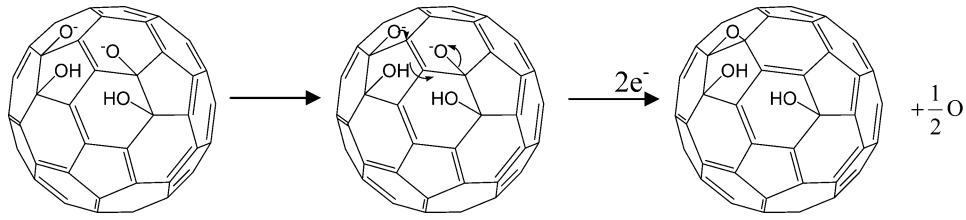

Scheme 2. Reaction mechanism for oxidation of fullerenol on anode surface.

$$2OH^- - 2e^- \Rightarrow H_2O + \frac{1}{2}O_2\uparrow \qquad (2)$$

As shown in Scheme 2, the oxidation on the working electrode consists of the two anodic oxygen evolution processes. The first process can lead to an increase of acidity at the anode, a reduction of the solubility of the reaction product, and the formation of a film on the surface.

CONCLUSION

In conclusion, a highly hydroxylated and negatively charged C_{60} has been synthesized by the electrophilic addition of sodium zincate in THF under strong basic conditions. In spite of being charged, fullerenol has a strong tendency to aggregate in solution with particle sizes of 50 nm in diameter. This derivatization provides fullerenol with an electromigration behavior in the same solution, which has been utilized to prepare fullerenol films. SEM results indicate that the film appearance and thickness are highly time-dependent. Current−time curves show that the deposition time dependence of the arrangement of fullerenol molecules on the surface is due to the decreased deposition rate and increased film resistance over time. Furthermore, FT-IR, XPS, and elemental analysis results reveal the characteristic features of fullerenol with a hemiketal structure for the film prepared by electrodeposition, and the stoichiometry of the film can be written as $C_{60}O(OH)_{12}$. The deposition mechanism has been further validated through electrochemical measurements and dissolved oxygen concentration testing to be an oxidation process, which consists of two stages of anodic oxygen evolution.

EXPERIMENTAL SECTION

Synthesis Method. Our synthesis technique is based upon the electrophilic property of sodium zincate under strong basic conditions. The freshly distilled THF was deoxygenated by purging with gaseous argon for at least 30 min. A small amount of solid C_{60} (150 mg; 99.9%, Strem Chemicals.Inc. Fullerenes) and THF (50 mL, Kermel Corporation) were placed in a vial and sonicated under very mild conditions (90 W, 40 kHz) for 1.5−2 h at room temperature. A reaction flask was charged with NaOH (0.12 g; Kermel Corporation), deionized water (20 mL), and excess Zn powder. Sodium zincate in the NaOH solution was synthesized in 30 min. Excess Zn solid was removed using a filter. Then, the aqueous NaOH solution, with dissolved sodium zincate, was added into the purple solution of C_{60} in THF. Finally, this C_{60} suspension in basic solution was sonicated under the same conditions for at least 3 h. During this reaction, the solution turned from purple to black. Furthermore, the solution can directly be utilized to prepare the fullerenol film in our paper. To improve the appearance of the film, a large solid was filtered off using a nylon membrane filter (nominal pore size 0.45 μm, Millipore).

The fullerenol was extracted from the solution using the reported method in refs 27 and 31. A precipitate was formed by adding acetonitrile and centrifuging the solution. It was washed and centrifuged twice with methanol and dried under vacuum for 2 days, and a brown powder was obtained. However, an aqueous solution of the sample still exhibited pH > 9, indicating incomplete removal of NaOH. Therefore, an additional purification step was a repeated diffusion dialysis process, carried out until the aqueous fullerenol solution with a pH at or below that of the deionized water was used to dissolve the sample. A brown solid product (178 mg/yield: 85%) was obtained by drying the concentrated fullerenol solution under reduced pressure. IR (KBr) ν: 3400, 1619, 1385, 1051, 775, 527 cm^{-1}; XPS At%: C 78.72, Na 2.65, O 18.62; Anal. Calcd for $C_{60}(OH)_{12}(ONa)_2$ wt %: C, 71.86; H, 1.20. Found: C, 71.48; H, 1.21. TOF MS *m/z*: 720 (C_{60}), 793 ($NaC_{60}O(OH)_2$), 817 ($C_{60}O_5(OH)$), 841 ($NaC_{60}O_4(OH)_2$), 865 ($Na_2C_{60}O_3(OH)_3$), 889 ($C_{60}O(OH)_9$), 913 ($Na_2C_{60}O_6(OH)_3$), 937 ($C_{60}O_4(OH)_9$), 961 ($NaC_{60}O_4(OH)_9$), 985 ($Na_2C_{60}O_2(OH)_{11}$). It is confirmed in this way the molecular formula of the fullerenol is $C_{60}(OH)_{12}(ONa)_2$ (MW = 1002 g mol^{-1}).

Characterization. The powder of fullerenol was directly compressed with potassium bromide and characterized by Fourier Transformation Intermediate Infrared System (EQUINOX55, BRUKER). The fullerenols were also characterized using an X-ray photoelectron spectrometer (K-Alpha, VG), CHNS/O element analyzer (EA3000, EURO) and a time of flight mass spectrometer (MALDI/TOF-TOF, BRUKER). TEM was done using TECNAIG2 microscope (PHILIPS), with sample solutions prepared with deionized water. The films on FTO conductive glass surfaces were examined using scanning electron microscopy (S-4800, Hitachi).

Electrochemical Experiments. The electrochemical characterization of fullerenol $C_{60}(OH)_{12}(ONa)_2$ in fullerenol/aqueous anode interface was carried out using a potentiostat/galvanostat system (SP 150, Bio-Logic SAS). The potentiostatic and cyclic voltammetric measurements were conducted in THF/aqueous NaOH solutions containing some dissolved sodium zincate (5:2 by volume) at room temperature. The constant voltage used for potentiostatic measurements was 10 V. The scan rate used for cyclic voltammetric measurements was 5 $mV \cdot s^{-1}$.

DO Concentration Measurement. The dissolved oxygen concentration was monitored using DO tester (InoLab Oxi Level 2, WTW). Experiments were conducted in THF/aqueous NaOH solutions containing dissolved sodium zincate (5:2 by volume) at room temperature, with and without fullerenol $C60(OH)_{12}(ONa)_2$. A FTO conductive glass and a platinum sheet were immersed in the prepared solutions as anode and cathode, respectively. The two solutions were deoxygenated by purging with gaseous argon before testing. Dissolved oxygen concentration was measured under the protection of argon, when a voltage of 10 V was supplied. Temperature was 28.9 °C.

REFERENCES AND NOTES

1. Rincón, M. E.; Hu, H.; Campos, J.; Ruiz-García, J. Electrical and Optical Properties of Fullerenol Langmuir-Blodgett

Films Deposited on Polyaniline Substrates. *J. Phys. Chem. B* **2003**, *107*, 4111–4117.
2. Injac, R.; Perse, M.; Obermajer, N.; Djordjevic-Milic, V.; Prijatelj, M.; Djordjevic, A.; Cerar, A.; Strukelj, B. Potential Hepatoprotective Effects of Fullerenol $C_{60}(OH)_{24}$ in Doxorubicin-Induced Hepatotoxicity in Rats with Mammary Carcinomas. *Biomaterials* **2008**, *29*, 3451–3460.
3. Jiao, F.; Liu, Y.; Qu, Y.; Li, W.; Zhou, G. Q.; Ge, C. C.; Li, Y. F.; Sun, B. Y.; Chen, C. Y. Studies on Anti-Tumor and Antimetastatic Activities of Fullerenol in a Mouse Breast Cancer Model. *Carbon* **2010**, *48*, 2231–2243.
4. Giacalone, F.; Martín, N. Fullerene Polymers: Synthesis and Properties. *Chem. Rev.* **2006**, *106*, 5136–5190.
5. Cao, T. B.; Yang, S. M.; Yang, Y. L.; Huang, C. H.; Cao, W. X. Photoelectric Conversion Property of Covalent-Attached Multilayer Self-Assembled Films Fabricated from Diazoresin and Fullerol. *Langmuir* **2001**, *17*, 6034–6036.
6. Rincón, M. E.; Guirado-López, R. A.; Rodríguez-Zavala, J. G.; Arenas-Arrocena, M. C. Molecular Films Based on Polythiophene and Fullerol: Theoretical and Experimental Studies. *Sol. Energy Mater. Sol. Cells* **2005**, *87*, 33–47.
7. Chaudhuri, P.; Paraskar, A.; Soni, S.; Mashelkar, R. A.; Sengupta, S. Fullerenol-Cytotoxic Conjugates for Cancer Chemotherapy. *ACS Nano* **2009**, *3*, 2505–2514.
8. Sitharaman, B.; Bolskar, R. D.; Rusakova, I.; Wilson, L. J. $Gd@C_{60}[C(COOH)_2]_{10}$ and $Gd@C_{60}(OH)_x$: Nanoscale Aggregation Studies of Two Metallofullerene MRI Contrast Agents in Aqueous Solution. *Nano Lett.* **2004**, *4*, 2373–2378.
9. Gharbi, N.; Pressac, M.; Hadchouel, M.; Szwarc, H.; Wilson, S. R.; Moussa, F. [60]Fullerene is a Powerful Antioxidant *In Vivo* with No Acute or Subacute Toxicity. *Nano Lett.* **2005**, *5*, 2578–2585.
10. Chiang, L. Y.; Lu, F. J.; Lin, J. T. Free Radical Scavenging Activity of Water-Soluble Fullerenols. *J. Chem. Soc., Chem. Commun.* **1995**, *12*, 1283–1284.
11. Cai, X. Q.; Jia, H. Q.; Liu, Z. B.; Hou, B.; Luo, C.; Feng, Z. H.; Li, W. X.; Liu, J. K. Polyhydroxylated Fullerene Derivative $C_{60}(OH)_{24}$ Prevents Mitochondrial Dysfunction and Oxidative Damage in an MPP1-Induced Cellular Model of Parkinson's Disease. *J. Neurosci. Res.* **2008**, *86*, 3622–3634.
12. Goswami, T. H.; Nandan, B.; Alam, S.; Mathur, G. N. A Selective Reaction of Polyhydroxy Fullerene with Cycloaliphatic Epoxy Resin in Designing Ether Connected Epoxy Star Utilizing Fullerene as a Molecular Core. *Polymer* **2003**, *44*, 3209–3214.
13. Chiang, L. Y.; Wang, L. Y.; Kuo, C. S. Polyhydroxylated C_{60} Cross-Linked Polyurethanes. *Macromolecules* **1995**, *28*, 7574–7576.
14. Ouyang, J. Y.; Zhou, S. Q.; Wang, F.; Goh, S. H. Structures and Properties of Supramolecular Assembled Fullerenol/Poly(dimethylsiloxane) Nanocomposites. *J. Phys. Chem. B* **2004**, *108*, 5937–5943.
15. Maruyama, R. Electrochemical Mass Flow Control of Hydrogen Using a Fullerene-Based Proton Conductor. *Electrochim. Acta* **2002**, *48*, 85–89.
16. Maruyama, R.; Shiraishi, M.; Hinokuma, K.; Yamada, A.; Ata, M. Electrolysis of Water Vapor Using a Fullerene-Based Electrolyte. *Electrochem. Solid-State Lett.* **2002**, *5*, A74–A76.
17. Chiang, L. Y.; Upasani, R. B.; Swirczewski, J. W. Versatile Nitronium Chemistry for C_{60} Fullerene Functionalization. *J. Am. Chem. Soc.* **1992**, *114*, 10154–10157.
18. Chiang, L. Y.; Upasani, R. B.; Swirczewski, J. W.; Soled, S. Evidence of Hemiketals Incorporated in the Structure of Fullerols Derived from Aqueous Acid Chemistry. *J. Am. Chem. Soc.* **1993**, *115*, 5453–5457.
19. Chiang, L. Y.; Swirczewski, J. W.; Hsu, C. S.; Chowdhury, S. K.; Cameron, S.; Creegan, K. Multi-Hydroxy Additions onto C_{60} Fullerence Molecules. *J. Chem. Soc., Chem. Commun.* **1992**, 1791–1793.
20. Chiang, L. Y.; Wang, L. Y.; Swirczewski, J. W.; Soled, S.; Cameron, S. Efficient Synthesis of Polyhydroxylated Fullerene Derivatives *via* Hydrolysis of Polycyclosulfated Precursors. *J. Org. Chem.* **1994**, *59*, 3960–3968.
21. Chen, B. H.; Huang, J. P.; Wang, L. Y.; Shiea, J.; Chen, T. L.; Chiang, L. Y. Facile Sulfation of C_{60} Using P_2O_5 as an Oxidation Promoter. *J. Chem. Soc., Perkin Trans. 1* **1998**, 1171–1174.
22. Chiang, L. Y.; Bhonsle, J. B.; Wang, L.; Shu, S. F.; Chang, T. M.; Hwu, J. R. Efficient One-Flask Synthesis of Water-Soluble [60]Fullerenols. *Tetrahedron* **1996**, *52*, 4963–4972.
23. Kokubo, K.; Matsubayashi, K.; Tategaki, H.; Takada, H.; Oshima, T. Facile Synthesis of Highly Water-Soluble Fullerenes More Than Half-Covered by Hydroxyl Groups. *ACS Nano* **2008**, *2*, 327–333.
24. Wang, S.; He, P.; Zhang, J. M.; Jiang, H.; Zhu, S. Z. Novel and Efficient Synthesis of Water-Soluble [60]Fullerenol by Solvent-Free Reaction. *Synth. Commun.* **2005**, *35*, 1803–1808.
25. Zhang, J. M.; Yang, W.; He, P.; Zhu, S. Z. Efficient and Convenient Preparation of Water-Soluble Fullerenol. *Chin. J. Chem.* **2004**, *22*, 1008–1011.
26. Alves, G. C.; Ladeira, L. O.; Righi, A.; Krambrock, K.; Calado, H. D.; Freitas Gil, R. P.; Pinheiro, M. V. B. Synthesis of $C_{60}(OH)_{18-20}$ in Aqueous Alkaline Solution Under O_2-Atmosphere. *J. Braz. Chem. Soc.* **2006**, *17*, 1186–1190.
27. Husebo, L. O.; Sitharaman, B.; Furukawa, K.; Kato, T.; Wilson, L. J. Fullerenols Revisited as Stable Radical Anions. *J. Am. Chem. Soc.* **2004**, *126*, 12055–12064.
28. Li, J.; Takeuchi, A.; Ozawa, M.; Li, X. H.; Saigo, K.; Kitazawa, K. C_{60} Fullerol Formation Catalysed by Quaternary Ammonium Hydroxides. *J. Chem. Soc., Chem. Commun.* **1993**, 1784–1785.
29. Troshin, P. A.; Astakhova, A. S.; Lyubovskaya, R. N. Synthesis of Fullerenols from Halofullerenes. *Fullerenes, Nanotubes, Carbon Nanostruct.* **2005**, *13*, 331–343.
30. Pinteala, M.; Dascalu, A.; Ungurenasu, C. Binding fullerenol $C_{60}(OH)_{24}$ to dsDNA. *Int. J. Nanomed.* **2009**, *4*, 193–199.
31. Vileno, B.; Marcoux, P. R.; Lekka, M.; Sienkiewicz, A.; Fehér, T.; Forró, L. Spectroscopic and Photophysical Properties of a Highly Derivatized C_{60} Fullerol. *Adv. Funct. Mater.* **2006**, *16*, 120–128.
32. Naim, A.; Shevlin, P. B. Reversible Addition of Hydroxide to the Fullerenes. *Tetrahedron Lett.* **1992**, *33*, 7097–7100.
33. Schneider, N. S.; Darwish, A. D.; Kroto, H. W.; Taylor, R.; Walton, D. R. M. Formation of Fullerols *via* Hydroboration of Fullerene-C_{60}. *J. Chem. Soc., Chem. Commun.* **1994**, 463–464.
34. Xing, G. M.; Zhang, J.; Zhao, W. L.; Tang, J.; Zhang, B.; Gao, X. F.; Yuan, H.; Qu, L.; Cao, W. B.; Chai, Z. F.; et al. Influences of Structural Properties on Stability of Fullerenols. *J. Phys. Chem. B* **2004**, *108*, 11473–11479.
35. Yang, X. C. *Master Thesis*, Capital Normal University, Beijing, China, 2003.
36. Kräschmer, W.; Lamb, L. D.; Fostiropoulos, K.; Huffman, D. R. Solid C_{60}: A New Form of Carbon. *Nature* **1990**, *347*, 354–357.
37. Brant, J. A.; Labille, J.; Robichaud, C. O.; Wiesner, M. Fullerol Cluster Formation in Aqueous Solutions: Implications for Environmental Release. *J. Colloid Interface Sci.* **2007**, *314*, 281–288.
38. Brant, J. A.; Labille, J.; Bottero, J. Y. Characterizing the Impact of Preparation Method on Fullerene Cluster Structure and Chemistry. *Langmuir* **2006**, *22*, 3878–3885.
39. Georgakilas, V.; Pellarini, F.; Prato, M.; Guldi, D. M.; Melle-Franco, M.; Zerbetto, F. Supramolecular Self-Assembled Fullerene Nanostructures. *Proc. Natl. Acad. Sci. U.S.A.* **2002**, *99*, 5075–5080.